Structural signatures of igneous sheet intrusion propagation

Craig Magee[a]*, James Muirhead[b], Nick Schofield[c], Richard J. Walker[d], Olivier Galland[e], Simon Holford[f], Juan Spacapan[g], Christopher A-L Jackson[a], William McCarthy[h]

[a]Basins Research Group, Department of Earth Science and Engineering, Imperial College London, London, SW7 2BP, UK

[b]Department of Geological Sciences, University of Idaho, Moscow, Idaho, 83844, USA

[c]Geology & Petroleum Geology, School of Geosciences, University of Aberdeen, Aberdeen, AB24 3UE, UK

[d]School of Geography, Geology, and the Environment, University of Leicester, Leicester, LE1 7RH, UK

[e]Physics of Geological Processes (PGP), The Njord Centre, Department of Geosciences, University of Oslo, Blindern, 0316 Oslo, Postbox 1048, Norway

[f]Australian School of Petroleum, University of Adelaide, Adelaide, SA 5005, Australia

[g]Universidad Nacional de La Plata-CONICET-Fundación YPF, 1900 La Plata, Argentina

[h]Department of Earth Sciences, University of St Andrews, St Andrews, KY16 9AL, UK

*corresponding author: c.magee@imperial.ac.uk (+44 (0)20 7594 6510)

Keywords: Magma; Sheet intrusion; Dyke; Sill; Flow; Structure

Abstract

The geometry and distribution of planar igneous bodies (i.e. sheet intrusions), such as dykes, sills, and inclined sheets, has long been used to determine emplacement mechanics, define melt source locations, and reconstruct palaeostress conditions to shed light on various

tectonic and magmatic processes. Since the 1970's we have recognised that sheet intrusions do not necessarily display a continuous, planar geometry, but commonly consist of segments. The morphology of these segments and their connectors is controlled by, and provide insights into, the behaviour of the host rock during emplacement. For example, tensile brittle fracturing leads to the formation of intrusive steps or bridge structures between adjacent segments. In contrast, brittle shear faulting, cataclastic and ductile flow processes, as well as heat-induced viscous flow or fluidization, promotes magma finger development. Textural indicators of magma flow (e.g., rock fabrics) reveal that segments are aligned parallel to the initial sheet propagation direction. Recognising and mapping segment long axes thus allows melt source location hypotheses, derived from sheet distribution and orientation, to be robustly tested. Despite the information that can be obtained from these structural signatures of sheet intrusion propagation, they are largely overlooked by the structural and volcanological communities. To highlight their utility, we briefly review the formation of sheet intrusion segments, discuss how they inform interpretations of magma emplacement, and outline future research directions.

1. Introduction

Igneous sheet intrusions are broadly planar bodies (e.g., dykes, sills, and inclined sheets) that facilitate magma flow through Earth's crust. The distribution and geometry of sheet intrusions is considered to be broadly controlled by the principal stress axes during emplacement, with intrusion walls typically orienting orthogonal to σ_3 within the σ_1-σ_2 plane, thus providing a record of syn-emplacement stress conditions (e.g., Anderson, 1936; Anderson, 1951; Gautneb and Gudmundsson, 1992; Rubin, 1995; Muirhead et al., 2015). Mapping and analysing the emplacement of igneous sheet swarms therefore allows volcano-tectonic processes to be unravelled, as well as aiding in identifying magma source locations and palaeogeographic reconstruction (e.g., Anderson, 1936; Walker, 1993; Ernst et al., 1995; Geshi, 2005). Overall, the link between intrusion geometry and contemporaneous stress field conditions has underpinned and dominated research and teaching of igneous sheet emplacement in the fields of structural geology and volcanology.

Over the last 50 years, it has been recognised that most igneous sheet intrusions consist of segments (e.g., Pollard et al., 1975; Delaney and Pollard, 1981; Rickwood, 1990; Schofield et al., 2012a), similar to structures observed in clastic intrusions (e.g., Vétel and Cartwright, 2010) and mineralized veins (e.g., Nicholson and Pollard, 1985). Most research has focused on segmented dykes emplaced via tensile elastic fracturing of the host rock (e.g., Delaney and Pollard, 1981; Rickwood, 1990). However, several studies have demonstrated that mechanisms other than tensile elastic fracturing, such as brittle shear faulting, ductile flow, and granular flow host rock deformation (e.g., fluidization), can also promote segmentation of sheet intrusions (e.g., Pollard et al., 1975; Hutton, 2009; Schofield et al., 2010; Spacapan et al., 2017). Segmentation of igneous sheets is documented over at least five orders of magnitude in scale, from intrusions that are a few centimetres to hundreds of meters thick, suggesting that segment formation and linkage are scale independent (Schofield et al., 2012a). Variable morphologies of segments (e.g., magma fingers; Pollard et al., 1975; Schofield et al., 2010), as well as those of potential connectors between segments (e.g., intrusive steps, broken bridges; Rickwood, 1990), characterise the broader sheet geometry and reflect the mechanical processes that facilitate emplacement (Schofield et al., 2012a). Rock fabric analyses of primary magma flow structures (e.g., chilled margin magnetic fabrics) have shown that the long axes of segments and their connectors are typically parallel to the direction of initial sheet propagation (e.g., Baer and Reches, 1987; Rickwood, 1990; Baer, 1995; Liss et al., 2002; Magee et al., 2012; Hoyer and Watkeys, 2017). Identification and analysis of segments and connectors in the field and in seismic reflection data thus provides a simple way to map primary magma propagation patterns and determine syn-emplacement host rock behaviour (e.g., Rickwood, 1990; Hansen et al., 2004; Thomson and Hutton, 2004; Trude et al., 2004; Schofield et al., 2012a; Schofield et al., 2012b). Here, our aim is to: (i) summarise our current understanding of magma segment formation and sheet intrusion; (ii) highlight how these structures can be used to unravel controls on magma flow through sheet intrusions in Earth's crust; and (iii) outline future research directions and implications for the study of sheet intrusion emplacement.

2. Primary magma flow indicators

2.1. Intrusive steps and bridge structures formed by tensile brittle fracturing

Regardless of their orientation or propagation direction, many sheet intrusions exhibit a stepped geometry consisting of sub-parallel segments that are slightly offset from one another and may overlap (Figs 1-3) (e.g., Delaney and Pollard, 1981; Rickwood, 1990; Schofield et al., 2012a). It is broadly accepted that stepped intrusion geometries result from segmentation of a propagating tensile elastic fracture, i.e. oriented orthogonal to σ_3, immediately ahead of an advancing sheet intrusion (e.g., Delaney and Pollard, 1981; Baer, 1995). As magma fills the fracture, segments begin to inflate and widen through lateral tip propagation, promoting tensile fracture of the intervening host rock and eventual segment coalescence (Fig. 1A) (e.g., Rickwood, 1990; Hutton, 2009; Schofield et al., 2012a). Structural signatures of this segmentation are controlled by segment offset, which describes the strike-perpendicular distance between the planes of two segments, and overlap, which can be negative (i.e. underlap) and describes the strike-parallel distance between segment tips (Fig. 1A) (cf. Delaney and Pollard, 1981; Rickwood, 1990). We also introduce 'stepping direction', which can either be consistent or inconsistent, to define the relative offset direction of adjacent segments (Fig. 1B).

Insert Figure 1

When viewed in a 2D cross-section (e.g., an outcrop), segments typically appear unconnected at their distal end, away from the magma source, whereas increased magma supply in proximal locations promotes their inflation and coalescence to form a continuous sheet intrusion (Fig. 1A) (Rickwood, 1990; Schofield et al., 2012a; Schofield et al., 2012b). Connectors between segments are classified as intrusive steps, if the segment overlap is neutral or negative, or bridge structures when segments overlap (Figs 1-3). Changes in overlap along segment long axes may mean steps transition into bridge structures and vice versa (Schofield et al., 2012a; Schofield et al., 2012b). Variations in the degree and style of segment connectivity with distance from the magma source imply that the segmentation process results from initial sheet propagation dynamics (Schofield et al., 2012a).

Insert Figures 2 and 3

2.1.1. Fracture segmentation

Two processes are commonly invoked to explain the development of initially unconnected fracture segments: (i) syn-emplacement rotation of the principal stress axes orientations (e.g., Pollard et al., 1982; Nicholson and Pollard, 1985; Takada, 1990); and (ii) exploitation of preferentially oriented, pre-existing structures (e.g., Hutton, 2009; Schofield et al., 2012a; Stephens et al., 2017). Geological systems likely display a combination of these segmentation mechanisms, and potentially others, so it is therefore important to understand the characteristics of each process to decipher their relative contributions.

In the first scenario, a change in the principal stress axes orientation ahead of a propagating fracture, likely due to the onset of mixed mode loading (mode I+II or mode I+III), causes it to twist and split into en-echelon segments that strike orthogonal to the locally reoriented σ_3 axis (Fig. 4A) (Pollard et al., 1982; Nicholson and Pollard, 1985; Cooke et al., 1999). This segmentation of mixed mode fractures is dictated by the maximum circumferential stress direction, direction of maximum energy release, maximum principal stress, direction of strain energy minimum, and the symmetry criterion (Cooke et al., 1999). The plane broadly defined by the overall geometry of the en-echelon segments remains parallel to the orientation of the original fracture (Fig 4A) (Rickwood, 1990). Steps and bridge structures generated due to this style of segmentation have a consistent stepping direction (e.g., Fig. 1B).

Insert Figure 4

The second mechanism for step and bridge formation involves exploitation of preferentially oriented (i.e. with respect to the contemporaneous principal stress axes), pre-existing structures by propagating fractures/intrusions (e.g., Hutton, 2009; Schofield et al., 2012a; Stephens et al., 2017). For example, many sills emplaced into sedimentary strata can be divided into segments that exploited different bedding planes in an attempt to find the least resistant pathway (e.g., Figs 2D and 3A) (Hutton, 2009). Bedding planes are particularly exploited because they: (i) exhibit relatively lower tensile strength and fracture toughness compared to intact rock (e.g., Schofield et al., 2012a; Kavanagh and Pavier, 2014; Kavanagh et al., 2017); and/or (ii) mark a significant mechanical contrast in intact rock properties (e.g., Poisson's ratio, Young's modulus) that localises strain (e.g., Kavanagh et al., 2006; Gudmundsson, 2011). In contrast to en-echelon segments, the stepping direction of intrusions exploiting different pre-existing weaknesses may be inconsistent (Figs 1B and 3E) (Schofield et al., 2012a).

Alternative mechanisms that may account for segmentation and step formation involve: (i) development of high stress intensities at the leading edge of an intruding sheet, promoting rapid crack propagation and formation of a fracture morphology, with a consistent stepping direction, akin to hackle marks (Fig. 4B) (Schofield et al., 2012a); or (ii) the occurrence of low or zero fracture toughness, pre-existing structures (e.g., faults), striking orthogonal to the sheet propagation direction, which can promote segmentation and provide a pathway for magma to form a fault-parallel step (Magee et al., 2013; Stephens et al., 2017). The stepping direction of sills influenced by pre-existing faults is controlled by the fault dip direction relative to the sheet propagation direction (Magee et al., 2013). In these scenarios, the stepped fracture plane is continuous and thus allows the magma to propagate as a single sheet; bridge structures cannot form via these processes because segments do not overlap (e.g., Fig. 1B).

2.1.2. Host rock deformation and bridge development

When segments overlap, their inflation may be accommodated by bending of the intervening host rock bridge (Figs 1A, 3A, and B) (Farmin, 1941; Nicholson and Pollard, 1985; Rickwood, 1990; Hutton, 2009). The monoformal folding of the host rock bridge records a tangential longitudinal strain relative to the orientation of the folded layers and induces outer-arc extension and inner-arc compression along the fold convex and concave surfaces, respectively (Hutton, 2009; Schofield et al., 2012a). As magma inflation continues, outer-arc extension increases and may exceed the tensile strength of the intact host rock, promoting development of extension fractures across the bridge (Figs 3B and C) (e.g., Hutton, 2009; Schofield et al., 2012b). Fractures cross-cutting unfolded bridge structures may also form if local crack-inducing stresses at segment tips are sufficiently high to promote fracture rotation and propagation towards each other (e.g., Fig. 3D) (e.g., Olson and Pollard, 1989). Continued fracture growth and infilling by magma can separate the bridge from one or both sides to form a broken bridge (Fig. 3B) or a bridge xenolith (Fig. 3D), respectively (Hutton, 2009).

2.2. Magma finger formation through brittle and/or non-brittle processes

In contrast to established tensile brittle fracturing models, several studies have demonstrated that magma may intrude via brittle faulting, cataclastic flow, or non-brittle processes (e.g., Pollard et al., 1975; Duffield et al., 1986; Schofield et al., 2010; Schofield et al., 2012a; Wilson et al., 2016). Such host rock deformation modes lead to the emplacement of magma fingers; i.e. long, linear or sinuous, narrow segments that have blunt and/or bulbous terminations (e.g., Pollard et al., 1975; Schofield et al., 2010; Schofield et al., 2012a; Spacapan et al., 2017).

Sheet intrusion into unconsolidated or highly incompetent host rocks, where little cohesion between grains and/or low shear moduli inhibits tensile brittle failure, can instigate magma finger formation (e.g., Pollard et al., 1975; Schofield et al. 2012a). For example, accommodation of magma by pore collapse and cataclastic flow can affect sheet intrusions emplaced: (i) at shallow-levels in sedimentary basins where host rock sequences have undergone little burial and/or diagenesis (e.g., Einsele et al., 1980; Morgan et al., 2008; Schofield et al., 2012a); or (ii) in strata that have been prevented from undergoing normal compaction with burial (Eide et al., 2017). Observed pegmatite bead-strings, which appear similar to magma fingers, formed during syn- or post-metamorphism and emplaced into hot, incompetent rocks suggests high ambient host rock temperatures can promote ductile host rock deformation and magma finger formation (cf. Bons et al., 2004).

Shear failure of unconsolidated and relatively soft (e.g., shale) host rock by brittle faulting and/or ductile deformation can also form and accommodate magma fingers (Fig. 5) (e.g., Pollard, 1973; Duffield et al., 1986; Rubin, 1993; Spacapan et al., 2017). For example, kinematic indicators of such compressional shear structures adjacent to magma fingers in the Neuquen Basin, Argentina, indicate that the intrusion 'pushed' into the host rock, leading to confined rock wedging (Fig. 5) (Pollard, 1973; Rubin, 1993; Spacapan et al., 2017). This hybrid propagation mechanism, called viscous indentation, is assumed to occur when the viscous shear stresses within a flowing magma, near its intrusion tip, are transferred to and promote shear failure of the host rock (Galland et al., 2014). Viscous indentation is therefore expected to primarily accommodate emplacement of viscous magma (Donnadieu and Merle, 1998; Merle and Donnadieu, 2000).

Insert Figure 5

Intrusion-induced heating (i.e. primary non-brittle emplacement) can cause some host rocks, particularly evaporites and bituminous coals, to behave as high viscosity fluids (i.e. fluidisation), the viscous deformation of which allows low viscosity melt injections to form magma fingers (e.g., Fig. 6) (Schofield et al., 2010; Schofield et al., 2012a; Schofield et al., 2014). Magma fingers can also form by fluidization (i.e. granular flow) of coherent, mechanically competent host rock (e.g., Pollard et al., 1975; Schofield et al. 2012a); i.e. secondary induced non-brittle magma emplacement (Schofield et al., 2012a). Two secondary induced non-brittle emplacement scenarios may be considered whereby magma intrusion can: (i) promote *in situ* boiling and volatisation of pore-fluids via heating (i.e. thermal fluidization); or (ii) open fractures that rapidly depressurize pore-fluids, which expand and catastrophically disaggregate the host rock (Schofield et al., 2010; Schofield et al., 2012a).

Insert Figure 6

3. Discussion

Having described how segmentation occurs and is structurally accommodated, here we discuss selected examples of how this knowledge has been applied and highlight possible future directions.

3.1. Lateral magma flow in mafic sill-complexes

The current paradigm describing crustal magma transport broadly involves the vertical ascent and/or lateral intrusion of dykes (e.g., Gudmundsson, 2006; Cashman and Sparks, 2013). However, recent field- and seismic-based studies that infer magma flow patterns from segment long axes and/or rock fabric analyses within interconnected networks of mafic sills and inclined sheets (i.e. sill-complexes), demonstrate that these systems can facilitate significant vertical (up to 12 km) and lateral (up to 4000 km) magma transport (e.g., Cartwright and Hansen, 2006; Leat, 2008; Muirhead et al., 2014; Magee et al., 2016). The lateral growth of such sill-complexes has been shown to control vent migrations and, potentially, transitions from effusive to explosive volcanism in active and extinct mafic monogenetic volcanic fields (e.g., Kavanagh et al., 2015; Muirhead et al., 2016). Mapping segment long axes suggests that sill-complexes may be as important as dykes in various tectonic, magmatic, and volcanic processes (Magee et al., 2016).

3.2. Intrusion opening vectors

Over a century of research has led to the prescribed dogma that sheet opening exclusively involves tensile dilation of Mode I fractures (e.g., Anderson, 1936). Intrusion planes are therefore expected to orient orthogonal to σ_3, which is a function of the interplay between far-field and local stress fields (e.g., Anderson, 1936; Anderson, 1951; Odé, 1957; Gautneb and Gudmundsson, 1992; Geshi, 2005). However, from analysing sheet segmentation processes, it is clear that several brittle and non-brittle processes can accommodate the emplacement of sheet intrusions that may not orient orthogonal to σ_3 (e.g., Schofield et al., 2012a; Schofield et al., 2014). Although often overlooked, it is therefore important to test the validity of the assumed relationship between the orientation of intrusive sheets and σ_3, through analysis of intrusion opening vectors (e.g., Walker, 1993; Jolly and Sanderson, 1997; Walker, 2016; Walker et al., 2017). Importantly, the geometry of segment connectors provides a record of local intrusion opening vectors (e.g., Olson and Pollard, 1989; Walker, 1993; Jolly and Sanderson, 1995; Cooke and Pollard, 1996; Stephens et al., 2017; Stephens et al., 2018). Steps formed during pure tensile opening of parallel magma segments should have virtually zero thickness and simply accommodate shear displacement on a plane orthogonal to the sheet intrusion plane (e.g., Figs 2A and C) (e.g., Stephens et al., 2017). Conversely, thick steps require an opening vector that was *not* orthogonal to the intrusion plane (e.g., Fig. 2D) (Walker et al., 2017). Whilst opening vectors of individual connectors may largely reflect local stress fields related to crack-tip processes (e.g., Olson and Pollard, 1989), identifying and collating such opening vector measurements across a sheet intrusion swarm can provide a more robust test of the syn-emplacement stress conditions than analyses of sheet orientation alone (Jolly and Sanderson, 1997; Walker et al., 2017). In particular, cataloguing opening vectors of segments within a sheet intrusion complex may help determine whether variably-oriented intrusions can be prescribed to single or multiple stress states. For example, although sill segments within the San Rafael Sub-Volcanic Field, USA range in dip from ~50° SE to

~40° NW, all record vertical opening vectors that indicate emplacement of the entire complex occurred within a single stress state (Stephens et al., 2018).

3.3. Bridge structures and relay zones

As with intrusions, faults and fractures grow through stages of nucleation and linkage of multiple discontinuous segments (e.g., Cartwright et al., 1996; Walsh et al., 2003). The amount of overlap and offset of fault or fracture segments, and the existence of pre-existing structure, leads to different styles of deformation in the intervening *relay zone* that accommodates displacement gradients between fault segments (e.g., Tentler and Acocella, 2010). Despite the apparent similarity of relay zones and bridge structures (Schofield et al., 2012b), few comparisons exist between the resulting ancillary structures associated with segmented faults and segmented intrusions. Whilst relay zones have received considerable attention in the literature (e.g., Peacock and Sanderson, 1991; Long and Imber, 2011), to our knowledge there is no catalogue of overlap, offset, and strain parameters for bridge structures. We suggest that systematic study of bridge structures, and comparison to relay zones, could yield important constraints on shared processes.

4. Conclusion

Igneous sheet intrusions are not necessarily emplaced as continuous, planar bodies but commonly develop through the coalescence of discrete magma segments. Segmentation can be primarily attributed to either: (i) splitting of a tensile brittle fracture propagating ahead of a sheet intrusion due to stress field rotations or exploitation of pre-existing weaknesses; (ii) brittle shear and flow (i.e. pore collapse) deformation of poorly consolidated host rocks; and/or (iii) non-brittle host rock fluidization. By briefly reviewing advances in our understanding of sheet intrusion growth, we demonstrate how different emplacement processes produce a variety of segment morphologies (e.g., magma fingers) and connecting structures (e.g., steps and bridge structures), the long axes of which record the initial fracture/magma propagation dynamics. We highlight how mapping of sheet segments and analysing their formation can provide important clues regarding the distribution of melt sources, how magma transits Earth's crust, mechanics of intrusion-induced host rock deformations, and palaeostress states in various volcanic-tectonic environments.

5. Acknowledgments

CM acknowledges a Junior Research Fellowship funded by Imperial College London. JDM acknowledges National Science Foundation grant EAR-1654518. Ken McCaffrey, Paul Bons, and Sandy Cruden are thanked for their constructive reviews.

6. Figure Captions

Figure 1: (A) Schematic diagram documenting the description and development of segments connected by steps and bridge structures (modified from Magee et al., 2016). Note the monoformal folding of bridge structures. (B) Schematic diagram defining consistent and inconsistent stepping directions.

Figure 2: Steps developed in mafic sheets intruding: (A and B) Mesozoic limestone and shale metasedimentary rocks on Ardnamurchan, NW Scotland; (C) Neoproterozoic schists at Mallaig, NW Scotland; and (D) a sedimentary succession on Axel Heiburg island, Canada (photo courtesy of Martin Jackson).

Figure 3: Different bridge structures recorded in mafic intrusions into: (A) Beacon Supergroup sedimentary strata along the Theron Mountains, Antarctica (modified from

Hutton, 2009); (B) Beacon Supergroup sedimentary strata along the Allan Hills, Antarctica; (C) a massive dolerite intrusion on Ardnamurchan, NW Scotland; and (D) Mesozoic limestone and shale metasedimentary rocks on Ardnamurchan, NW Scotland. (E) Opacity render of a sill in the Flett Basin, NE Atlantic and corresponding seismic sections detailing intrusive step and bridge growth along i-iv segment boundaries (modified from Schofield et al., 2012b); note that it can be difficult to determine where segments are bounded by steps or bridge structures in seismic reflection data.

Figure 4: (A) Schematic showing how a change in the principal stress axes can segment a propagating sheet (after Hutton, 2009). (B) Hackle marks developed on a joint plane (redrawn from Kulander et al., 1979).

Figure 5: Small-scale imbricate fold and thrust duplex developed due to viscous indentation of finger-like sill intrusions in the Neuquén Basin, Argentina (modified from Spacapan et al., 2017).

Figure 6: (A and B) Magma fingers developed in response to intrusion-induced heating and plastic deformation of the host rock coals in the Raton Basin, Colorado (modified from Schofield et al., 2012a). (C) Schematic diagrams showing the simplified 3D morphology of the magma fingers in (A and B) (Schofield, 2009).

7. References

Anderson, E.M., 1936. Dynamics of formation of cone-sheets, ring-dykes, and cauldron subsidence. Proceedings of the Royal Society of Edinburgh 56, 128-157.

Anderson, E.M., 1951. The dynamics of faulting and dyke formation with applications to Britain. Oliver and Boyd, Edinburgh, 206 pp.

Baer, G., 1995. Fracture propagation and magma flow in segmented dykes: field evidence and fabric analyses, Makhtesh Ramon, Israel. Physics and chemistry of dykes. Balkema, Rotterdam, 125-140.

Baer, G., Reches, Z.E., 1987. Flow patterns of magma in dikes, Makhtesh Ramon, Israel. Geology 15, 569-572.

Cartwright, J.A., Hansen, D.M., 2006. Magma transport through the crust via interconnected sill complexes. Geology 34, 929-932.

Cartwright, J.A., Mansfield, C., Trudgill, B., 1996. The growth of normal faults by segment linkage. In: Buchanan, P.G., Nieuwland, D.A., (eds), Modern Developments in Structural Interpretation, Validation and Modelling. Geological Society, London, Special Publications 99, 163-177.

Cashman, K.V., Sparks, R.S.J., 2013. How volcanoes work: A 25 year perspective. Geological Society of America Bulletin 125, 664-690.

Cooke, M.L., Mollema, P.N., Pollard, D.D., Aydin, A., 1999. Interlayer slip and joint localization in the East Kaibab Monocline, Utah: field evidence and results from numerical modelling. Geological Society, London, Special Publications 169, 23-49.

Cooke, M.L., Pollard, D.D., 1996. Fracture propagation paths under mixed mode loading within rectangular blocks of polymethyl methacrylate. Journal of Geophysical Research: Solid Earth 101, 3387-3400.

Delaney, P.T., Pollard, D.D., 1981. Deformation of host rocks and flow of magma during growth of minette dikes and breccia-bearing intrusions near Ship Rock, New Mexico. US Geological Survey Professional Paper 1202, 61 pp.

Donnadieu, F., Merle, O., 1998. Experiments on the indentation process during cryptodome intrusions: new insights into Mount St. Helens deformation. Geology 26, 79-82.

Duffield, W.A., Bacon, C.R., Delaney, P.T., 1986. Deformation of poorly consolidated sediment during shallow emplacement of a basalt sill, Coso Range, California. Bull Volcanol 48, 97-107.

Eide, C.H., Schofield, N., Jerram, D.A., Howell, J.A., 2017. Basin-scale architecture of deeply emplaced sill complexes: Jameson Land, East Greenland. Journal of the Geological Society 174, 23-40.

Einsele, G., Gieskes, J.M., Curray, J., Moore, D.M., Aguayo, E., Aubry, M.-P., Fornari, D., Guerrero, J., Kastner, M., Kelts, K., 1980. Intrusion of basaltic sills into highly porous sediments, and resulting hydrothermal activity. Nature 283, 441-445.

Ernst, R., Head, J., Parfitt, E., Grosfils, E., Wilson, L., 1995. Giant radiating dyke swarms on Earth and Venus. Earth-Science Reviews 39, 1-58.

Farmin, R., 1941. Host-rock inflation by veins and dikes at Grass Valley, California. Economic Geology 36, 143-174.

Galland, O., Burchardt, S., Hallot, E., Mourgues, R., Bulois, C., 2014. Dynamics of dikes versus cone sheets in volcanic systems. Journal of Geophysical Research: Solid Earth 119, 6178-6192.

Gautneb, H., Gudmundsson, A., 1992. Effect of local and regional stress fields on sheet emplacement in West Iceland. Journal of Volcanology and Geothermal Research 51, 339-356.

Geshi, N., 2005. Structural development of dike swarms controlled by the change of magma supply rate: the cone sheets and parallel dike swarms of the Miocene Otoge igneous complex, Central Japan. Journal of Volcanology and Geothermal Research 141, 267-281.

Gudmundsson, A., 2006. How local stresses control magma-chamber ruptures, dyke injections, and eruptions in composite volcanoes. Earth-Science Reviews 79, 1-31.

Gudmundsson, A., 2011. Deflection of dykes into sills at discontinuities and magma-chamber formation. Tectonophysics 500, 50-64.

Hansen, D.M., Cartwright, J.A., Thomas, D., 2004. 3D seismic analysis of the geometry of igneous sills and sill junction relationships. In: Davies, R.J., Cartwright, J.A., Stewart, S.A., Lappin, M., Underhill, J.R., (eds), 3D seismic technology: Application to the exploration of sedimentary basins, Geological Society, London, Memoirs 29, 199-208.

Hoyer, L., Watkeys, M.K., 2017. Using magma flow indicators to infer flow dynamics in sills. Journal of Structural Geology 96, 161-175.

Hutton, D.H.W., 2009. Insights into magmatism in volcanic margins: bridge structures and a new mechanism of basic sill emplacement - Theron Mountains, Antarctica. Petroleum Geoscience 15, 269-278.

Jolly, R., Sanderson, D., 1997. A Mohr circle construction for the opening of a pre-existing fracture. Journal of Structural Geology 19, 887-892.

Jolly, R., Sanderson, D.J., 1995. Variation in the form and distribution of dykes in the Mull swarm, Scotland. Journal of Structural Geology 17, 1543-1557.

Kavanagh, J.L., Boutelier, D., Cruden, A., 2015. The mechanics of sill inception, propagation and growth: Experimental evidence for rapid reduction in magmatic overpressure. Earth and Planetary Science Letters 421, 117-128.

Kavanagh, J.L., Menand, T., Sparks, R.S.J., 2006. An experimental investigation of sill formation and propagation in layered elastic media. Earth and Planetary Science Letters 245, 799-813.

Kavanagh, J.L., Pavier, M.J., 2014. Rock interface strength influences fluid-filled fracture propagation pathways in the crust. Journal of Structural Geology 63, 68-75.

Kavanagh, J.L., Rogers, B.D., Boutelier, D., Cruden, A.R., 2017. Controls on sill and dyke-sill hybrid geometry and propagation in the crust: The role of fracture toughness. Tectonophysics 698, 109-120.

Kulander, B.R., Barton, C.C., Dean, S.L., 1979. Application of fractography to core and outcrop fracture investigations. Department of Energy, Morgantown, WV (USA). Morgantown Energy Research Center.

Leat, P.T., 2008. On the long-distance transport of Ferrar magmas. Geological Society, London, Special Publications 302, 45-61.

Liss, D., Hutton, D.H., Owens, W.H., 2002. Ropy flow structures: A neglected indicator of magma-flow direction in sills and dikes. Geology 30, 715-718.

Long, J.J., Imber, J., 2011. Geological controls on fault relay zone scaling. Journal of Structural Geology 33, 1790-1800.

Magee, C., Jackson, C.A.-L., Schofield, N., 2013. The influence of normal fault geometry on igneous sill emplacement and morphology. Geology 41, 407-410.

Magee, C., Muirhead, J.D., Karvelas, A., Holford, S.P., Jackson, C.A., Bastow, I.D., Schofield, N., Stevenson, C.T., McLean, C., McCarthy, W., 2016. Lateral magma flow in mafic sill complexes. Geosphere 12, 809-841.

Magee, C., Stevenson, C., O'Driscoll, B., Schofield, N., McDermott, K., 2012. An alternative emplacement model for the classic Ardnamurchan cone sheet swarm, NW Scotland, involving lateral magma supply via regional dykes. Journal of Structural Geology 43, 73-91.

Merle, O., Donnadieu, F., 2000. Indentation of volcanic edifices by the ascending magma. In: Vendeville, B., Mart, Y., Vigneresse, J.-L., (eds), Salt, Shale and Igneous Diapirs in and around Europe. Geological Society, London, Special Publications 174, 43-53.

Morgan, S., Stanik, A., Horsman, E., Tikoff, B., de Saint Blanquat, M., Habert, G., 2008. Emplacement of multiple magma sheets and wall rock deformation: Trachyte Mesa intrusion, Henry Mountains, Utah. Journal of Structural Geology 30, 491-512.

Muirhead, J.D., Airoldi, G., White, J.D., Rowland, J.V., 2014. Cracking the lid: Sill-fed dikes are the likely feeders of flood basalt eruptions. Earth and Planetary Science Letters 406, 187-197.

Muirhead, J.D., Kattenhorn, S.A., Le Corvec, N., 2015. Varying styles of magmatic strain accommodation across the East African Rift. Geochemistry, Geophysics, Geosystems 16, 2775-2795.

Muirhead, J.D., Van Eaton, A.R., Re, G., White, J.D., Ort, M.H., 2016. Monogenetic volcanoes fed by interconnected dikes and sills in the Hopi Buttes volcanic field, Navajo Nation, USA. Bulletin of Volcanology 78, 11.

Nicholson, R., Pollard, D., 1985. Dilation and linkage of echelon cracks. Journal of Structural Geology 7, 583-590.

Odé, H., 1957. Mechanical Analysis of the Dike Pattern of the Spanish Peaks Area, Colorado. Geological Society of America Bulletin 68, 567.

Olson, J., Pollard, D.D., 1989. Inferring paleostresses from natural fracture patterns: A new method. Geology 17, 345-348.

Peacock, D., Sanderson, D., 1991. Displacements, segment linkage and relay ramps in normal fault zones. Journal of Structural Geology 13, 721-733.

Pollard, D.D., 1973. Derivation and evaluation of a mechanical model for sheet intrusions. Tectonophysics 19, 233-269.

Pollard, D.D., Muller, O.H., Dockstader, D.R., 1975. The form and growth of fingered sheet intrusions. Geological Society of America Bulletin 86, 351-363.

Pollard, D.D., Segall, P., Delaney, P.T., 1982. Formation and interpretation of dilatant echelon cracks. Geological Society of America Bulletin 93, 1291-1303.

Rickwood, P., 1990. The anatomy of a dyke and the determination of propagation and magma flow directions. In: Parker, A.J., Rickwood, P.C., Tucker, D.H., (eds), Mafic dykes and emplacement mechanisms, Balkema, Rotterdam, 81-100.

Rubin, A.M., 1993. Tensile fracture of rock at high confining pressure: implications for dike propagation. Journal of Geophysical Research: Solid Earth 98, 15919-15935.

Rubin, A.M., 1995. Propagation of magma-filled cracks. Annual Review of Earth and Planetary Sciences 23, 287-336.

Schofield, N., 2009. Linking sill morphology to emplacement mechanisms. PhD thesis. University of Birmingham.

Schofield, N., Alsop, I., Warren, J., Underhill, J.R., Lehné, R., Beer, W., Lukas, V., 2014. Mobilizing salt: Magma-salt interactions. Geology 42, 599-602.

Schofield, N., Heaton, L., Holford, S.P., Archer, S.G., Jackson, C.A.-L., Jolley, D.W., 2012b. Seismic imaging of 'broken bridges': linking seismic to outcrop-scale investigations of intrusive magma lobes. Journal of the Geological Society 169, 421-426.

Schofield, N., Stevenson, C., Reston, T., 2010. Magma fingers and host rock fluidization in the emplacement of sills. Geology 38, 63-66.

Schofield, N.J., Brown, D.J., Magee, C., Stevenson, C.T., 2012a. Sill morphology and comparison of brittle and non-brittle emplacement mechanisms. Journal of the Geological Society 169, 127-141.

Spacapan, J.B., Galland, O., Leanza, H.A., Planke, S., 2017. Igneous sill and finger emplacement mechanism in shale-dominated formations: a field study at Cuesta del Chihuido, Neuquén Basin, Argentina. Journal of the Geological Society 174, 422-433.

Stephens, T.L., Walker, R.J., Healy, D., Bubeck, A., England, R., McCaffrey, K., 2017. Igneous sills record far-field and near-field stress interactions during volcano construction: Isle of Mull, Scotland. Earth and Planetary Science Letters 478, 159-174.

Stephens, T.L., Walker, R.J., Healy, D., Bubeck, A., England, R.W., 2018. Mechanical models to estimate the paleostress state from igneous intrusions. Solid Earth (in press).

Takada, A., 1990. Experimental study on propagation of liquid-filled crack in gelatin: Shape and velocity in hydrostatic stress condition. Journal of Geophysical Research: Solid Earth 95, 8471-8481.

Tentler, T., Acocella, V., 2010. How does the initial configuration of oceanic ridge segments affect their interaction? Insights from analogue models. Journal of Geophysical Research: Solid Earth 115, B01401.

Thomson, K., Hutton, D., 2004. Geometry and growth of sill complexes: insights using 3D seismic from the North Rockall Trough. Bulletin of Volcanology 66, 364-375.

Trude, K.J., 2004. Kinematic Indicators for Shallow Level Igneous Intrusions from 3D Seismic Data: Evidence of Flow Firection and Feeder Location. In: Davies, R.J., Cartwright, J.A., Stewart, S.A., Lappin, M., Underhill, J.R., (eds), 3D seismic technology: Application to the exploration of sedimentary basins, Geological Society, London, Memoirs 29, 209-218.

Vétel, W., Cartwright, J., 2010. Emplacement mechanics of sandstone intrusions: insights from the Panoche Giant Injection Complex, California. Basin Research 22, 783-807.

Walker, G.P.L., 1993. Re-evaluation of inclined intrusive sheets and dykes in the Cuillins volcano, Isle of Skye. In: Pritchard, H.M., Alabaster, T., Harris, N.B., Neary, C.R., (eds), Magmatic Processes and Plate Tectonics, Geological Society, London, Special Publications 76, 489-497.

Walker, R., Healy, D., Kawanzaruwa, T., Wright, K., England, R., McCaffrey, K., Bubeck, A., Stephens, T., Farrell, N., Blenkinsop, T., 2017. Igneous sills as a record of horizontal shortening: The San Rafael subvolcanic field, Utah. Geological Society of America Bulletin 129, 1052-1070.

Walker, R.J., 2016. Controls on transgressive sill growth. Geology 44, 99-102.

Walsh, J., Bailey, W., Childs, C., Nicol, A., Bonson, C., 2003. Formation of segmented normal faults: a 3-D perspective. Journal of Structural Geology 25, 1251-1262.

Wilson, P.I., McCaffrey, K.J., Wilson, R.W., Jarvis, I., Holdsworth, R.E., 2016. Deformation structures associated with the Trachyte Mesa intrusion, Henry Mountains, Utah: Implications for sill and laccolith emplacement mechanisms. Journal of Structural Geology 87, 30-46.

Figure 1

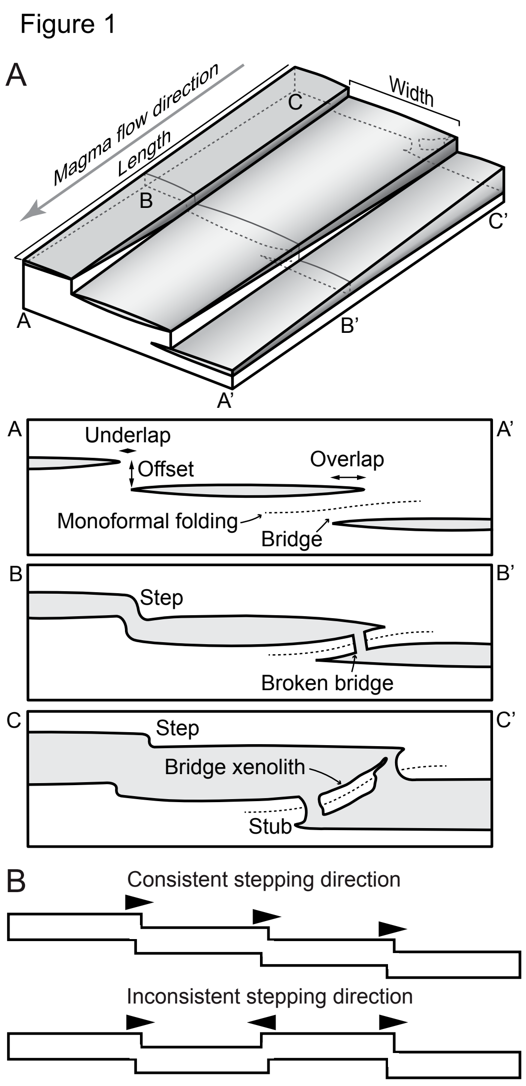

Figure 1: (A) Schematic diagram documenting the description and development of segments connected by steps and bridge structures (redrawn from Magee et al., 2016). (B) Schematic diagram defining consistent and inconsistent stepping directions.

Figure 2 colour

Figure 2

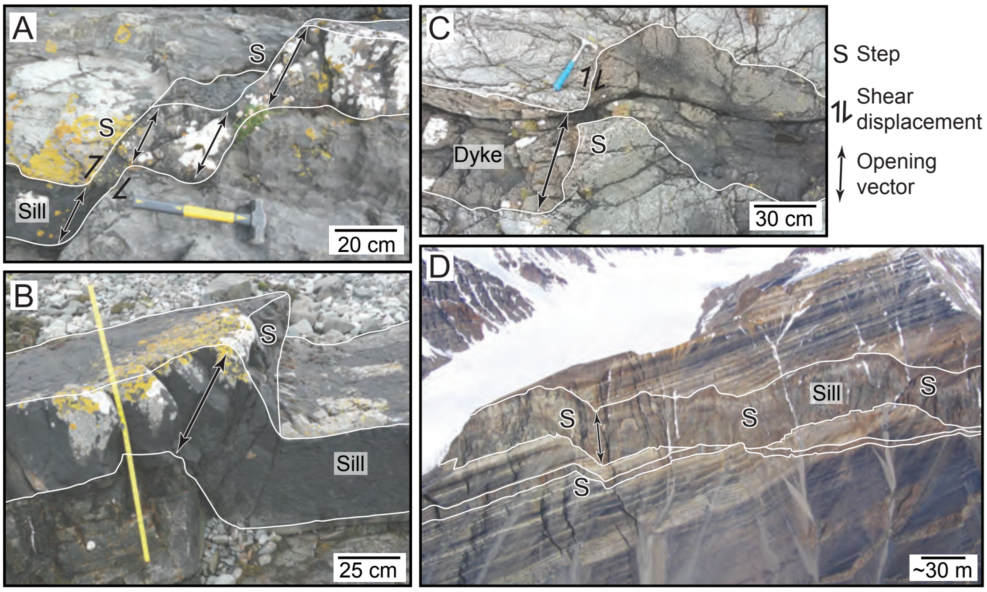

Figure 2: Steps developed in mafic sheets intruding: (A and B) Mesozoic limestone and shale metasedimentary rocks on Ardnamurchan, NW Scotland; (C) Neoproterozoic schists at Mallaig, NW Scotland; and (D) a sedimentary succession on Axel Heiburg island, Canada (photo courtesy of Martin Jackson).

Figure 3 colour

Figure 3

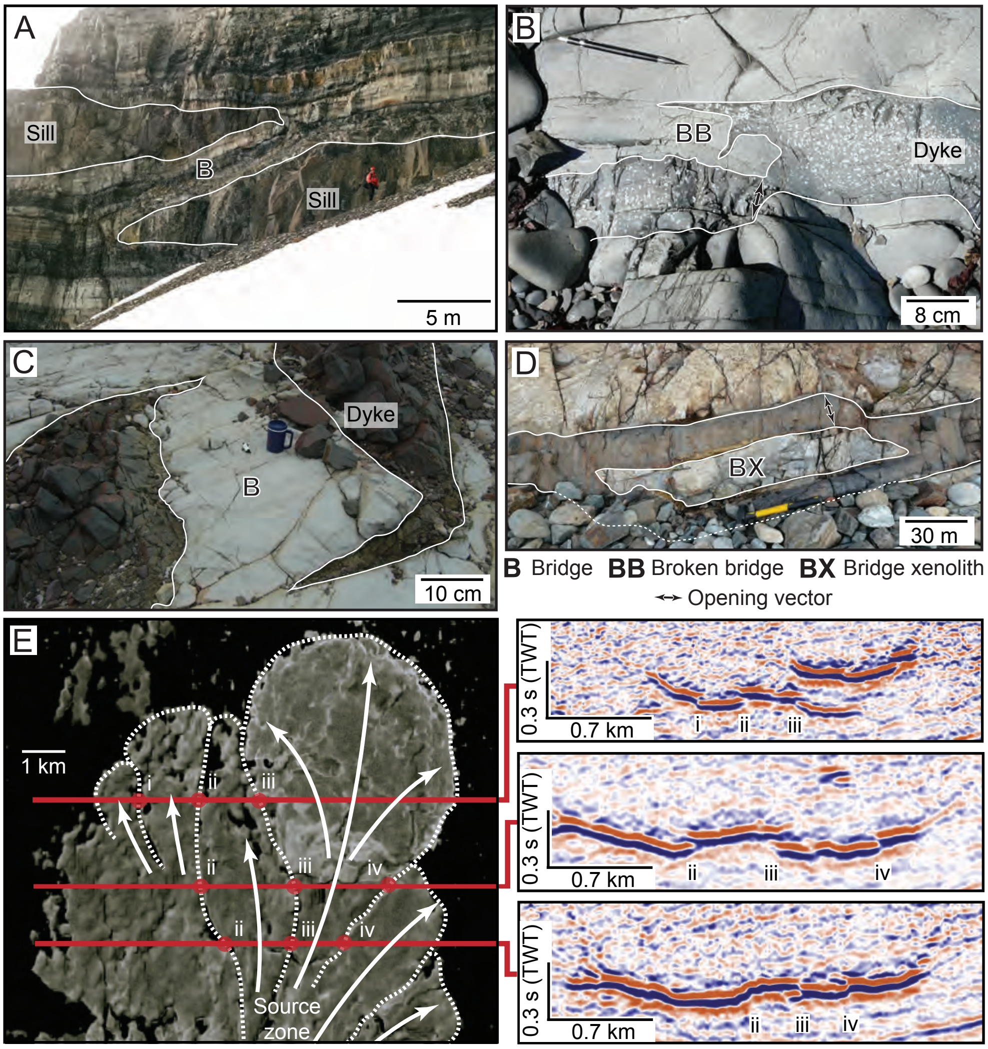

Figure 3: Different bridge structures recorded in mafic intrusions into: (A) Beacon Supergroup sedimentary strata along the Theron Mountains, Antarctica (modified from Hutton, 2009); (B) Beacon Supergroup sedimentary strata along the Allan Hills, Antarctica; (C) a massive dolerite intrusion on Ardnamurchan, NW Scotland; and (D) Mesozoic limestone and shale metasedimentary rocks on Ardnamurchan, NW Scotland. (E) Opacity render of a sill in the Flett Basin, NE Atlantic and corresponding seismic sections detailing intrusive step and bridge growth along i-iv segment boundaries (modified from Schofield et al., 2012b); note that it can be difficult to determine where segments are bounded by steps or bridge structures in seismic reflection data.

Figure 4

Figure 4

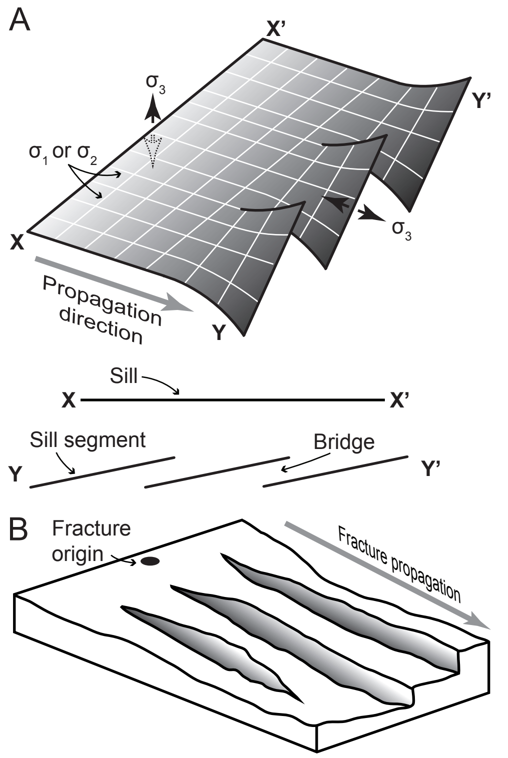

Figure 4: (A) Schematic showing how a change in the principal stress axes can segment a propagating sheet (after Hutton, 2009). (B) Hackle marks developed on a joint plane (redrawn from Kulander et al., 1979).

Figure 5 colour

Figure 5

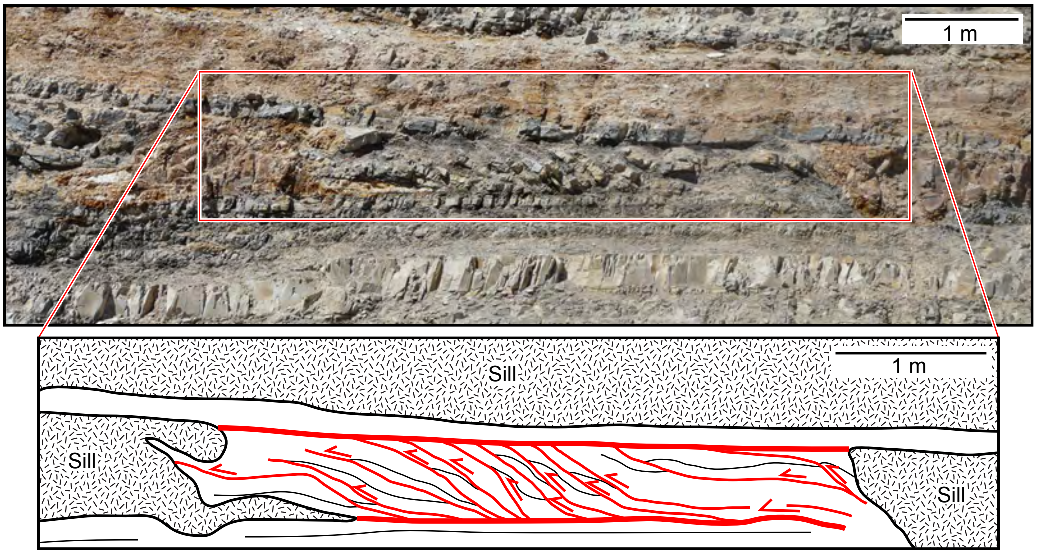

Figure 5: Small-scale imbricate fold and thrust duplex developed due to viscous indentation of finger-like sill intrusions in the Neuquén Basin, Argentina (modified from Spacapan et al., 2017).

Figure 6 colour

Figure 6

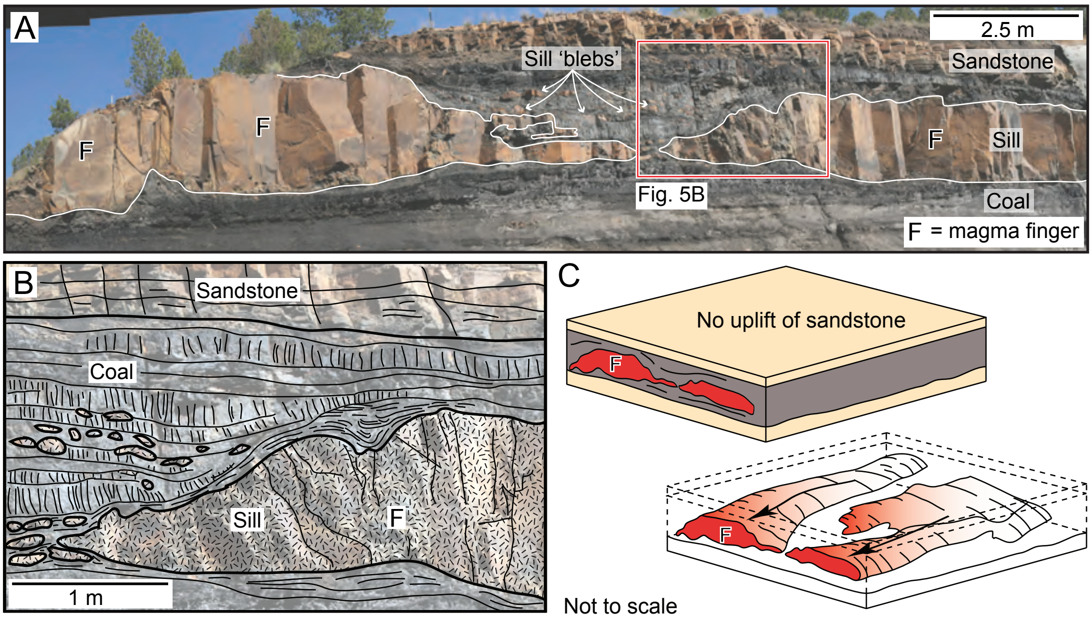

Figure 6: (A and B) Magma fingers developed in response to intrusion-induced heating and plastic deformation of the host rock coals in the Raton Basin, Colorado (modified from Schofield et al., 2012a). (C) Schematic diagrams showing the simplified 3D morphology of the magma fingers in (A and B) (Schofield, 2009).